Acta Mechanica Solida Sinica, Vol. 24, No. 2, April, 2011 ISSN 0894-9166
Published by AMSS Press, Wuhan, China

THE UNIQUE PROPERTIES OF THE SOLID-LIKE CONFINED LIQUID FILMS: A LARGE SCALE MOLECULAR DYNAMICS SIMULATION APPROACH**, ***

Fengchao Wang **Yapu Zhao***

(*State Key Laboratory of Nonlinear Mechanics, Institute of Mechanics, Chinese Academy of Sciences, Beijing* 100190*, China*)

Received 8 September 2010, revision received 20 March 2011

ABSTRACT The properties of the confined liquid are dramatically different from those of the bulk state, which were reviewed in the present work. We performed large-scale molecular dynamics simulations and full-atom nonequilibrium molecular dynamics simulations to investigate the shear response of the confined simple liquid as well as the n-hexadecane ultrathin films. The shear viscosity of the confined simple liquid increases with the decrease of the film thickness. Apart from the well-known ordered structure, the confined n-hexadecane exhibited a transition from 7 layers to 6 in our simulations while undergoing an increasing shear velocity. Various slip regimes of the confined n-hexadecane were obtained. Viscosity coefficients of individual layers were examined and the results revealed that the local viscosity coefficient varies with the distance from the wall. The individual n-hexadecane layers showed the shear-thinning behaviors which can be correlated with the occurrence of the slip. This study aimed at elucidating the detailed shear response of the confined liquid and may be used in the design and application of micro- and nano-devices.

KEY WORDS confined liquid, solid-like, shear-thinning, slip, large scale molecular dynamics simulation

I. INTRODUCTION

As is known to us all, a liquid is a kind of fluid that can flow and take the shape of a container. In contrast to the solid, the liquid can only be subjected to normal, compressive stresses, i.e., it can resist compression and it would continually deform under an applied shear stress, which can be found in any textbook of fluid mechanics[1]. When the liquid is confined in a narrow gap at the nanometer scale, referred to as the confined liquid[2], the motion of the liquid molecules will be strongly restricted by the potential resulting from solid wall. As a consequence, the properties of the confined liquid become dramatically different from those of the bulk state. The new dynamic behaviors of the confined liquid include: the density oscillations near the solid walls[3,4], the enhanced effective shear viscosity[5,6], the prolonged relaxation time[2], the transition to solidification[7,8], the reduced diffusion coefficient[9], etc. These solid-like properties cannot be simply understood according to the classical theory of the bulk liquid.

* Corresponding author. E-mail: yzhao@imech.ac.cn

** Project supported by the National Natural Science Foundation of China (NSFC, Nos. 60936001 and 11072244), the National Basic Research Program of China (973 Program, No. 2007CB310500) and the Shanghai Supercomputer Center.

*** This paper is an invited paper for cerebrating the 30th Anniversary of Acta Mechanica Solida Sinica

Indeed, understanding of the properties of the confined liquid has been arousing extensive interest from many research fields such as the fabrication of microelectromechanical systems (MEMS) and biochemical lab-on-a-chip systems[10], chemistry[11,12], polymer industry[13], tribology and lubrication[7].

Since 1990s, experiments using the surface force apparatus (SFA)[5–8] and atomic force microscope (AFM)[14,15] have led to many detailed studies and interesting results about the confined liquid. The liquid film usually contains only 6-10 molecule layers or even less, thence there is so little material to study[2]. Many researchers also turned to molecular dynamics (MD) simulations[16,17] as an alternative approach since MD simulations can provide clear insights into the liquid configuration as well as the fluid transport and are capable of revealing the properties of the confined liquids on the nanometer scale.

There have been numerous studies of the strong density oscillations of confined liquid at the liquid-solid interface based on SFA experiments[2,3] and MD simulations[17], which revealed the ordered structures of the liquid films. The density oscillations at the interface are resulted from the short-distance interactions between surfaces, which are called the solvation forces or structural forces[18]. When water is considered, these interactions are referred to as hydration forces[19,20]. More recently, a number of researchers moved forward to investigate the influence of the layering structures on the shear properties of the confined films. Yamada studied the behavior of confined polydimethylsiloxane (PDMS) under shear and found that the friction of the confined PDMS film abruptly increases when the film is compressed to a thickness of two molecule layers from four. This layering transition was attributed to the shear induced orientation of polymer molecules[21]. Using nonequilibrium molecular dynamics (NEMD) simulations, Jabbarzadeh et al. demonstrated the existence of a very low friction state of a six-layer dodecane film confined between mica surfaces under a constant pressure, accompanied with a sudden decrease of the film thickness[22]. The high viscosity state of the confined liquid was ascribed to the crystal bridge formations of the dodecane molecules[23]. Experimentally, the confinement rate effects were also examined[6,24]. Rapid quench resulted in less ordered layering, hence slip between layers of fluid molecules was impeded, manifesting a viscosity enhancement; and vice versa[6]. Bureau found that the confinement rate influenced the structure and the shear behavior of the liquid film with a thickness below 10 nm. Besides, the results indicated that this disordered film formed by the rapid quench is in a metastable state[24].

Viscosity is one of the fundamental properties of liquid, which indicates resistance to flow. Since the local viscosity coefficients could not be measured using the current experimental apparatus, an effective viscosity, which was achieved by the average over the width of the film, was used when examining the viscosity of the confined liquid. It was found that the effective shear viscosity of the confined liquid are much higher than that of the bulk liquid[5,6], which was interpreted as the collective motion of the liquid molecules due to the confinement. The confined liquid exhibited shear-thinning behavior, in which the viscosity decreases with increasing shear rate, both in SFA experiments[2] and MD simulations[16,25]. However, behaviors of individual liquid layers under shear, including structural orientation, sliding motion and the corresponding viscosity are relatively rare in recent literatures.

The fluidity of the confined liquid can be described with the Deborah number[26]. The Deborah number is a dimensionless number defined as $\mathrm{De} = t_{\mathrm{relaxation}}/t_{\mathrm{observation}}$, which is the ratio of the relaxation time and the characteristic time scale of an observation (experiment or computer simulation). If $\mathrm{De} >> 1$, the material behaves as solid; If $\mathrm{De} << 1$, the material is an ordinary viscous fluid; If $\mathrm{De} \sim 1$, the material is of the intermediate state. Another similar dimensionless number is the Weissenberg number, $\mathrm{We} = \dot{\gamma}\tau$, which is the shear rate times the relaxation time[27]. The longer the relaxation time, the larger the Deborah number is, thus the confined liquid would appear to be more solid-like. For the bulk dodecane, the longest relaxation time is shorter than 10^{-10} s. However, the relaxation time of the confined dodecane is observed to be approximately 5×10^{-2} s, which is 10^8 times longer than in the bulk state[2]. The existence of the constrained molecular motions in the confined liquid is commonly invoked as the likely explanation for the dramatic increase of the relaxation time[15]. Since the relaxation time of the confined liquid is orders of magnitude longer than that of the bulk liquid, the corresponding De could show a transition from the fluid regime ($\mathrm{De} << 1$) to the intermediate regime ($\mathrm{De} \sim 1$), or even the solid regime ($\mathrm{De} >> 1$), thus the solid-like behaviors emerge. There has been controversy about the origin of solidification of the confined liquid. Some experimental data proved that it is a first-order transition from liquid-like to solid-like behavior, which means that solidification represents crystallization induced

by confinement[7,28]. However, others suggested it is a continuous glasslike transition instead[8]. Recent AFM and SFA experiments reported the results which are inconsistent with the abrupt first-order transition[29,30]. These findings added the new evidence to support the viewpoint that the confinement leads towards to a glasslike transition[31].

As mentioned previously, the density profiles of the confined liquid oscillate with distance perpendicular to the solid walls, extending several molecular diameters into the liquid[18]. The dynamic structure of the confined liquid parallel to the solid walls is still controversial. It has been suggested that the collective motion of the liquid molecules is characterized by the activation volume, which is defined as $\Delta V_{\rm act} = \Delta E/\Delta P_{\perp}$, where ΔE is the energy difference and $\Delta P_{\perp}$ is the net differential normal pressure[2]. It was demonstrated that the activation volume of the confined dodecane is about 20∼80 nm^3, varied with the shear rate, while in the bulk the value is smaller than 0.03 nm^3. The Fluorescence Correlation Spectroscopy (FCS) within an SFA was used to investigate the diffusion properties of the confined liquid

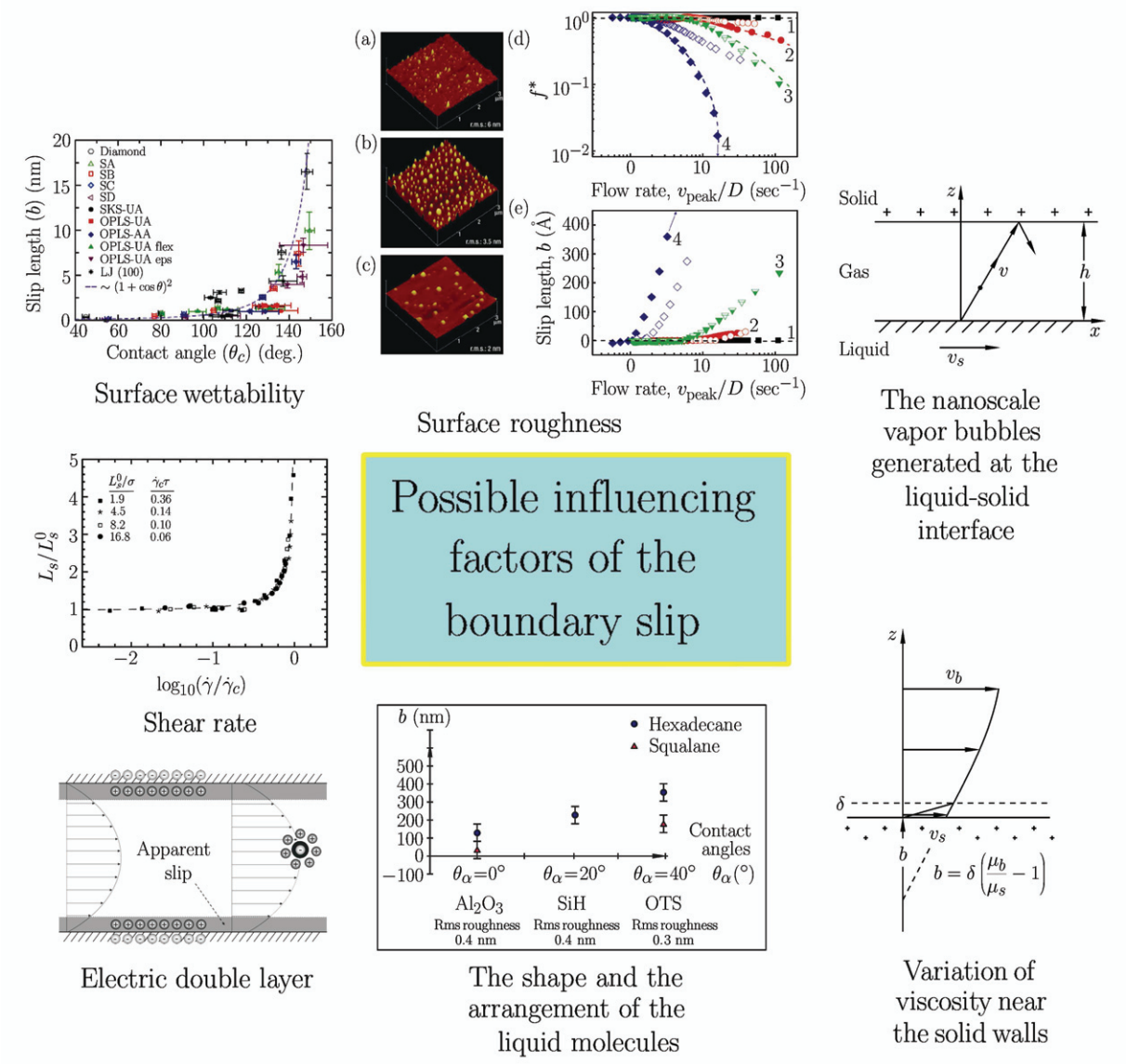

Fig. 1. Possible influencing factors of the boundary slip: the wettability of the solid surface[32], surface roughness[33], the nanoscale vapor bubbles generated at the liquid-solid interface[34], shear rate[35], the electric double layer[36], the shape and the arrangement of the liquid molecules[37], variation of viscosity near the solid walls[38].

films[9]. The activation volume for diffusion exceeds that of the bulk liquid by 3 orders of magnitude. The confinement of the solid walls also has influence on the diffusion of the confined liquid. The diffusion coefficient decreases exponentially from the edges towards the center of the contact area. These results associated with the collective motion of the liquid molecules indicate the lateral ordering of the confined liquid[9].

The mechanism of the slip at the liquid-solid interface and between the layers of the confined liquid is of particular importance for the understanding of the shear response of the confined ultrathin films. The boundary slip is dependent on various factors, such as the wettability of the solid surface[32], surface roughness[33], the nanoscale vapor bubbles generated at the liquid-solid interface[34], shear rate[35], the electric double layer[36], the shape and the arrangement of the liquid molecules[37], variation of viscosity near the solid walls[38], as summarized in Fig.1. For the slip of the confined liquid, Jabbarzadeh et al. used a united atoms model in MD simulations to study the influence of wall properties on the slip between hexadecane film and the walls[39,40]. Pit et al. probed the velocity of hexadecane within 80 nm from the solid wall and gave the direct experimental evidence of slip[41]. Zhu and Granick found that the amount of slip depended strongly on shear velocity. They proposed that the fluid viscosity might depend on distance from the wall[42].

In the present study, the dramatically different properties of the confined liquid were reviewed. As the film thickness comes to the nanometer scale, the confinement of the solid walls and the unique structures at the liquid-solid interface have a significant influence on the dynamic properties of the confined ultrathin liquid film. The enhanced effective shear viscosity and the reduced diffusion coefficient are owing to the slow relaxation process of the confined liquid. In contrast to the bulk liquid, the confined liquid behaves as the solid-like material due to the solidification. Brief comparisons of the confined liquid and the bulk liquid were summarized in Table 1. To explain more details about the dynamical process of the confined liquid under shear, two kinds of representative liquid were investigated with large-scale MD and NEMD approach. One is the simple liquid and the other is the *n*-hexadecane. The rest of the paper is organized as follows. In §II, simulation methodology and the necessary theoretical background were described

Table 1. **Brief comparisons of the confined liquid and the bulk liquid**

	Confined liquid	Bulk liquid
Molecular orientation	density oscillations (perpendicular to the walls); the lateral ordering (parallel to the walls).	short-range order. The package of the liquid molecules is much smaller than the crystal grain of the solid.
Effective shear viscosity	roughly several orders of magnitude larger than that of the bulk liquid, and increases with the decrease of the film thickness.	0.997×10^{-3}Pa·s (water, 293 K) 1.34×10^{-3}Pa·s (dodecane, 298 K)
Shear-rate dependence of viscosity	shear-thinning: the reduced viscosity can be observed when the shear rate exceeds certain critical value.	independent of the shear rate up to shear rate $> 10^{10}$ s^{-1} (dodecane)
Relaxation time	larger than 5×10^{-2} s, which exceeds that of the bulk liquid by 8 orders of magnitude.	less than 10^{-10} s
Activation volume	3 orders of magnitude larger than that of the bulk liquid.	smaller than 0.03 nm^3 (dodecane)
Diffusion coefficient	inhomogeneous (parallel to the walls)	
State of the substance	solid-like, fluid-like, and the transition between the two states. solidification.	liquid

briefly; in §III, we presented our MD results related to the shear response of the confined simple liquid as well as the n-hexadecane ultrathin films, mainly focused on the confinement induced structures, the film thickness dependent of the shear viscosity, the sliding motion between individual liquid layers and the corresponding shear-thinning behaviors; in §IV, we summarized the main conclusions and discussed the future work.

II. COMPUTATIONAL DETAILS

The MD simulations presented in this manuscript consist of two parts. The first one is the Couette flow of the confined simple liquid. Besides, the n-hexadecane confined between two Au walls was also studied. All the simulations in this study were performed using the parallelized MD code LAMMPS[43].

The confined simple liquid was represented by Lennard-Jones (LJ) particles which were confined between two Silicon walls containing 11 layers of atoms based on the diamond crystal structures. The solid walls were set to be parallel to the XY plane. The liquid was filled in a cubic geometry with edge length of L_X which was equal to the length of the simulation box. To investigate the effect of the thickness effect of the confined liquid, a series of MD simulations with different film thickness were carried out. The thickness of the liquid ranges from several angstroms to more than 140 nm and the total number of the atoms used in our simulations ranges from several thousands to 102 millions. To the best of our knowledge, we have performed the largest MD simulation of the in China in the community of fluid mechanics.

The interactions between the liquid and solid were modeled with the LJ potential

$$E_{\mathrm{LJ}} = 4\varepsilon_{\mathrm{LJ}}\left[\left(\frac{\sigma}{r}\right)^{12} - \left(\frac{\sigma}{r}\right)^{6}\right] \tag{1}$$

in which σ is the value of r where the potential is zero and $\varepsilon_{\mathrm{LJ}}$ determines the energetic scale of the pair interaction. The parameters for the liquid-liquid interaction were the same as that for the oxygen-oxygen interactions in the simple point charge water model[44]. The cutoff for these LJ interactions was set to be 10.0 Å.

After an energy minimization, each system was thermally equilibrated at 300.0 K for 0.2 ns using a Nose-Hoover thermostat[45] while the solid walls were treated to be rigid. Then the planar Couette flow was induced by moving the solid walls at equal velocity (1.0 Å/ps) in opposite directions along X axis so that the shear was applied in the XZ plane. The equations of motion were solved using a velocity-Verlet algorithm with a time step of 2.0 fs. To obtain the density profile, as shown in Fig.2, the simulation box was divided into N slices along Z direction and the density of each slice was calculated and averaged over a time duration of 1.0 ns. The velocity profile was acquired in a similar way.

In our full-atom NEMD simulations, a total number of 100 molecules of n-hexadecane were confined between two Au walls which were parallel to the XY plane. Each wall was composed of 800 Au atoms forming four (100) layers based on its known face center cubic crystal structures. The dimensions of the simulation box were $L_X = L_Y = 40.80$ Å and $L_Z = 46.47$ Å. Periodic boundary conditions were imposed in X and Y directions to minimize the edge effects.

The adaptive intermolecular reactive empirical bond order (AIREBO) potential[46], which is based on the widely used second-generation Brenner potential, was used to model the atomic interactions in the confined n-hexadecane system. The potential can be expressed by the following form:

$$E = \frac{1}{2}\sum_{i}\sum_{j\neq i}\left(E_{ij}^{\mathrm{REBO}} + E_{ij}^{\mathrm{LJ}} + \sum_{k\neq i,j}\sum_{l\neq i,j,k} E_{kijl}^{\mathrm{TORSION}}\right) \tag{2}$$

where i, j, k and l are the atom indices. The three terms in the square brackets represent covalent bonding interactions, LJ term, and torsion interactions, respectively. The REBO term describes the short-ranged interactions and the cutoff parameter was set to be 2.0 Å. The LJ term adds longer-ranged (2.0 Å$< r <$10.2 Å) interactions using a form similar to the standard LJ potential and has a cutoff of 10.2 Å. The TORSION term is an explicit 4-body potential that describes various dihedral angle preferences in hydrocarbon configurations.

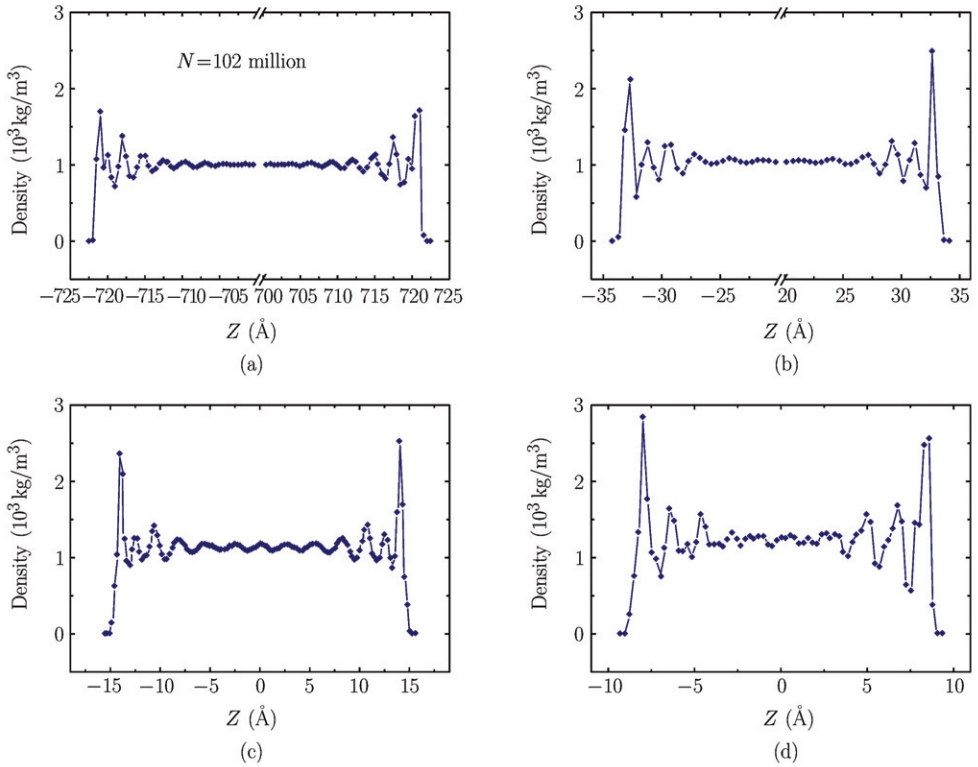

Fig. 2. Density profiles of the confined simple liquid at various film thickness: (a) 144.4 nm, (b) 6.24 nm, (c) 3.11 nm and (d) 1.86 nm.

The interactions between the n-hexadecane molecules and the Au walls were described by the classical 12-6 LJ potential. We used the Lorentz-Berthelot mixing rules to estimate the intermolecular potential parameters between the heteroatomic pairs of C-Au and H-Au, which were listed in Table 2, as well as the Au-Au LJ parameters[47]. The original LJ parameters for C and H came from the consistent-valence forcefield[48]. A cutoff distance of 10.0 Å was used for these LJ interactions.

Table 2. **LJ parameters for interactions between the n-hexadecane molecules and the Au walls**

	ε(Kcal/mol)	σ(Å)
C-Au	0.630	3.256
H-Au	0.621	2.543
Au-Au	10.180	2.637

The initial configuration of n-hexadecane was obtained from an energy minimization. After that, simulations were carried out in the NVT ensemble to thermally equilibrate the system at 300.0 K for 2.0 ns with a time step of 1.0 fs while keeping the Au atoms fixed, namely, the film thickness was kept constant. Then the Couette flow simulations were performed using a procedure similar to what we used for the confined simple liquid. To study the shear response of the confined n-hexadecane film, a series of shear velocity between 0.01 and 50.0 Å/ps were imposed. In each case, NEMD simulations were performed for another 2.0 ns from the equilibrium state for data production. To exclude the thermal noise effect and induce an appreciable flow velocity profile, these shear velocities are high compared to that imposed in experiments. As a consequence, the confined liquid was heated up during the shear, so significant kinetic-energy rescaling is required to remove the generated heat. In our simulations, only the Y and Z velocity components were taken into account when calculating the temperature of the n-hexadecane system.

III. RESULTS AND DISCUSSIONS

3.1. Density Oscillations Near the Confining Solid Walls

In Fig.2, we plotted the density profiles of the confined liquid at different thickness according to the MD simulations. These results can illustrate several important points. First, the density oscillations concentrate near the liquid-solid interface, in the range of 4-8 molecular diameters, higher near solid walls and lower at the middle part of the film. For large thickness of the confined liquid, the trends of the oscillation are not as clear in the middle. The density of this region is uniform and approximately equals to that of the bulk liquid. While for small thickness, the ordered liquid layers seem to occupy the whole channel. Second, as the film thickness decreases, the confinement induces more strong ordered structures at the interface. It can be observed in Fig.2 that the density of the first three layers adjacent to solid walls increases along with the reduced film thickness. Finally, the period of the oscillation roughly equals to the dimension of a liquid molecule. The density oscillations were resulted from the attractive interfacial interactions and the geometric constraining effect[18]. Particularly, the normal force along Z direction is an oscillatory function of distance, varying between attraction and repulsion[3]. And the force profiles were also observed to oscillate with a repeat spacing corresponding to the molecular dimensions in our MD simulations.

Some characteristic lengths can be introduced when considering the structure of the confined liquid and its dynamic properties. There are two relevant dimensionless numbers for such problem: the Hamaker number and the Ohnesorge number. The Hamaker number, $\mathrm{Ha} = A/\left(\pi\gamma a^2\right)$, is a dimensionless number defined as a measure of the ratio of van der Waals forces to surface tension[49]. The molecular length[50] can be derived from the Hamaker number as follows:

$$a = \sqrt{\frac{A}{6\pi\gamma}} \tag{3}$$

where A is the Hamaker constant and γ is the surface tension. Typically, a is of the order of several angstroms, which roughly equals to the period of the density oscillations. The critical film thickness[51]

$$e_0 = \frac{\eta^2}{\gamma\rho} \tag{4}$$

below which the viscous dissipation becomes dominant, can be derived from the Ohnesorge number[52], $\mathrm{Oh} = \eta/\sqrt{\rho\gamma L}$, which is a dimensionless number that relates the viscous forces to inertial and surface tension forces. If $\mathrm{Oh} > 1$, the viscous dissipation is dominant, then we obtain $L < e_0$.

Having presented some results about the liquid structures, we now discuss the influence of the density oscillation on the theoretical modeling of the confined liquid. The density should be a continuous function of the distance in the continuum fluid mechanics treatment. As the density oscillations were observed at the liquid-solid interface, the density is no longer a differentiable function of the distance, thus the validity of continuum theory becomes questionable. Although the linear velocity profile can be obtained in the MD simulations of the planar Couette flow, as the prediction of the Navier-Stokes equations, the first layer adjacent to solid walls behave very differently from the bulk liquid[53]. Based on our MD simulation results, if the thickness of the confined liquid is larger than 20 molecular diameters, the confined liquid can be divided into the bulk region and the interfacial region. The continuum mechanics treatment is still valid in the bulk region, and a connection should be founded between the two regions. If the thickness is less than 10 molecular diameters, the ordered structures near the interfaces would be strongly overlapped, which implies the inhomogeneous molecular mobility and the layering order in the whole film. Thus a new theoretical approach is required to give a better understanding of the unique dynamic properties of the confined liquid.

3.2. Viscosity of the Simple Liquid Dependent on the Thickness

The shear viscosity, as defined in Newton's law of viscosity, describes the resistance of a fluid to shear forces, which can also be related to momentum transport under the influence of velocity gradients. In our simulations, the shear viscosity was estimated from the steady-state average of the shear stress according to

$$\eta = \frac{\langle \tau_{XZ} \rangle}{\dot{\gamma}} \tag{5}$$

where τ_{XZ} is the XZ component of the stress tensor and $\dot{\gamma} = \partial v_X / \partial Z$ is the shear rate. For steady shear flows such as the planar Couette flow, the velocity profile can be obtained in MD simulations and used to analyze the shear rate. Stress tensor components of the confined liquid films were calculated from the virial theorem by the Irving-Kirkwood method, which took the form of

$$\tau_{\alpha\beta} = -\frac{1}{\Omega}\left(\sum_i m_i v_{i\alpha} v_{i\beta} + \frac{1}{2}\sum_i \sum_{j \neq i} F_{ij\alpha} r_{ij\beta}\right) \tag{6}$$

in which the subscripts α and β denote the Cartesian components which can be simply substituted by X, Y or Z. The summation of i is over all the atoms occupying the volume of the liquid film indicated by Ω. The contribution of each atom to the stress tensor is in two parts, a kinetic part and a configuration part. The first term in the square brackets is a kinetic energy contribution, where m_i is the mass of atom i, $\nu_{i\alpha}$ and $\nu_{i\beta}$ are the velocity components of atom i in the α and β directions, respectively. The second term represents a potential energy contribution. $F_{ij\alpha}$ is the α component of the force between atoms i and j along α axis, and $r_{ij\beta}$ is the projection of the inter-atomic distance vector along coordinate β.

To test the accuracy of Eq.(6), we calculated τ_{XZ} of the confined liquid with another approach. The force exerted on the wall by the liquid in the X direction was time averaged during the last 0.5 ns of the shear simulations. Then τ_{XZ} was obtained by dividing the force by the area of the wall. The relative error is less than 5.0% for all the cases. Therefore we also employed the method derived from Eqs.(5) and (6) to calculate the viscosity of individual layers of the confined n-hexadecane which will be discussed later.

We evaluated the shear viscosity of the confined liquid at different thickness, which was plotted in Fig.3. It can be found that the effect of decreasing thickness on the shear viscosity was not obvious until the thickness was reduced to 30 Å, then the shear viscosity increased rapidly. This critical value of the thickness of the confined liquid film is approximately two times of the range of the density oscillation extension at the liquid-solid interface. This enhanced shear viscosity indicated that the overlap of the layering structures at the liquid-solid interface has a significant influence on the dynamic properties of the confined liquid.

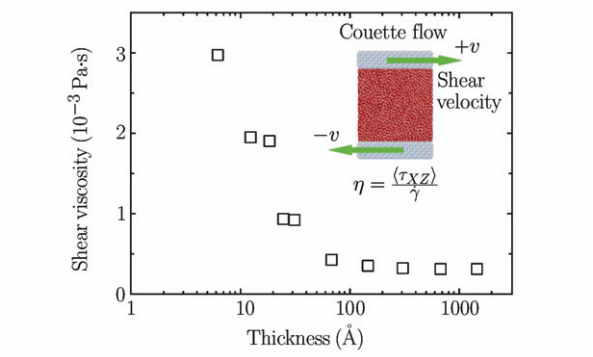

Fig. 3. Shear viscosity of the confined simple liquid versus the film thickness. Sketch of the MD simulations for the planar Couette flow was illustrated. The shear velocity is set to be 1 Å/ps.

3.3. Shear Induced Ordered Structure of the Confined *n*-hexadecane

The n-hexadecane is a straight chain alkane consisting of 16 carbon atoms and has a length of $\sim$ 24 Å and width of $\sim$ 4 Å. The bulk n-hexadecane appears as a colorless liquid under the usual condition and the melting temperature is 291 K. The n-hexadecane used in this study has an average density of 0.769 g/cm^3. In our simulations, the oscillatory density profile of the confined n-hexadecane under the equilibrium state is illustrated as the blue solid line in Fig.4, reflecting that there were 7 layers between

the two Au walls. For the convenience of the following indication, these layers were numbered from 1 to 7. The two Au walls were also marked as 0 and 8. The thickness of each layer approximately equals to the width of the n-hexadecane molecule, indicating that the confined n-hexadecane molecules were aligned to parallel to the Au walls. In contrast, simulation with periodic boundary conditions applied to Z direction was performed to mimic the bulk n-hexadecane liquid and the density profile was also calculated, as the red dash line shown in Fig.4. The large density fluctuation near the solid walls can be explained by the strong liquid-solid interactions.

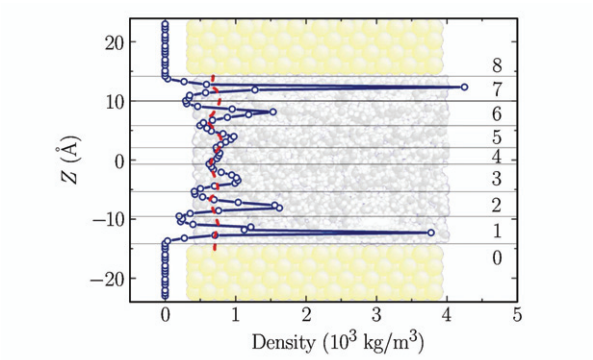

Fig. 4. Snapshot of the equilibrated configuration of the n-hexadecane films confined between two Au walls, processed by Atomeye[54]. The density profile of the system along the Z axis is given (blue solid line). The points which represent the density of the Au layers are removed for clarity. In contrast, periodic boundary conditions were applied to Z direction to mimic the bulk n-hexadecane liquid and the density profile was calculated (red dash line). The horizontal lines indicate the division of different liquid layers, which were numbered from 1 to 7 for the convenience of the following indication, and the two Au walls were also marked as 0 and 8.

In Fig.5, we presented the density and velocity profiles of the n-hexadecane liquid under shear. Four representative profiles are shown for the shear velocities of 0.1, 0.5, 5, and 50 Å/ps, respectively. Comparing the density profiles of the confined n-hexadecane liquid under different shear velocities, we can obtain two discernible results. First, the peak density of the liquid layers adjacent the confining walls is lowered as increasing the shear velocity. Besides, a transition of the number of n-hexadecane layers was observed in our simulations as the shear velocity increases. At relatively low shear velocity, there are 7 layers, while at high shear velocity there are only 6. This layering transition indicated that the ordered alignment of confined liquid molecules has been enhanced by the shear. The analogous result was obtained in a simulation of confined n-dodecane film between mica surfaces[39]. However, in that work, the separation between the mica walls was allowed to change under a fixed normal load, while the separation was fixed in our cases. Our results showed that the shearing action plays a dominant role in this alignment enhancement.

To investigate more details about the layering structure of the confined films, the order parameter was introduced, which were calculated using the equation

$$S_\alpha = \frac{3}{2}\left\langle \cos^2 \theta_\alpha \right\rangle - \frac{1}{2} \tag{7}$$

where the subscript α denotes the Cartesian component which can be X, Y or Z. θ_α is the angle between the α axis of the simulation box and the chord vector which connects every other pair of carbon atoms in a same molecule[55], shown in the upper inset of Fig.6. The order parameter can range from -0.5 (full order perpendicular to α axis) to 1.0 (full order parallel to α axis), with a value of 0 in the case of isotropic orientation (see the lower inset in Fig.6).

The order parameter S_Z was calculated during the simulations to examine the average orientation of the confined n-hexadecane. The results are presented in the lower panel of Fig.6. It can be clearly seen that tendency of the n-hexadecane molecules to align parallel to the Au walls becomes stronger as the shear velocity increases from 0.01 Å/ps to 5.0 Å/ps. These results are consistent with the first direct experimental measurement of shear-induced ordering of nano-confined films[56]. We can also see

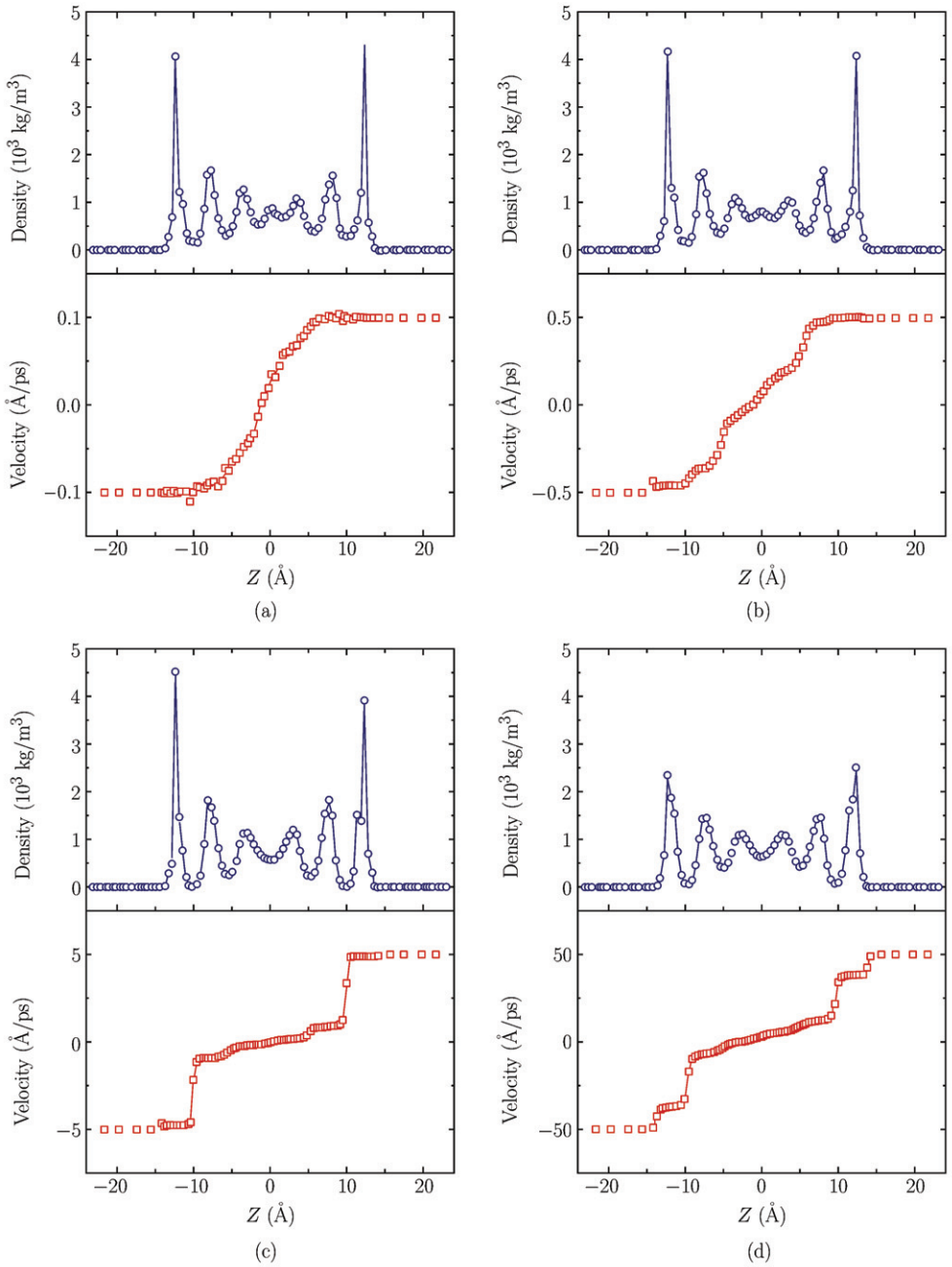

Fig. 5. Local density profile (open squares and blue lines) and velocity profile (open circles and red lines) of four representative shear velocities: (a) 0.1 Å/ps, (b) 0.5 Å/ps, (c) 5 Å/ps and (d) 50 Å/ps. The four points at either end of the velocity curve indicate the velocity of the four layers of Au atoms while the points which represent the density of the Au layers are removed for clarity.

an increment of S_Z when the shear velocity is even higher. As mentioned previously, shear induces the enhancement of the alignment of confined liquid molecules, so a layering transition takes place. As a result, the average occupying volume of each layer increases with the shear velocity, therefore, S_Z increases slightly with the decrease of the constraining effect of the solid wall. S_X, which quantifies how the n-hexadecane molecules prefer to parallel to the direction of flow, exhibits similar variation tendency as S_Z, implying the layering transition discussed above.

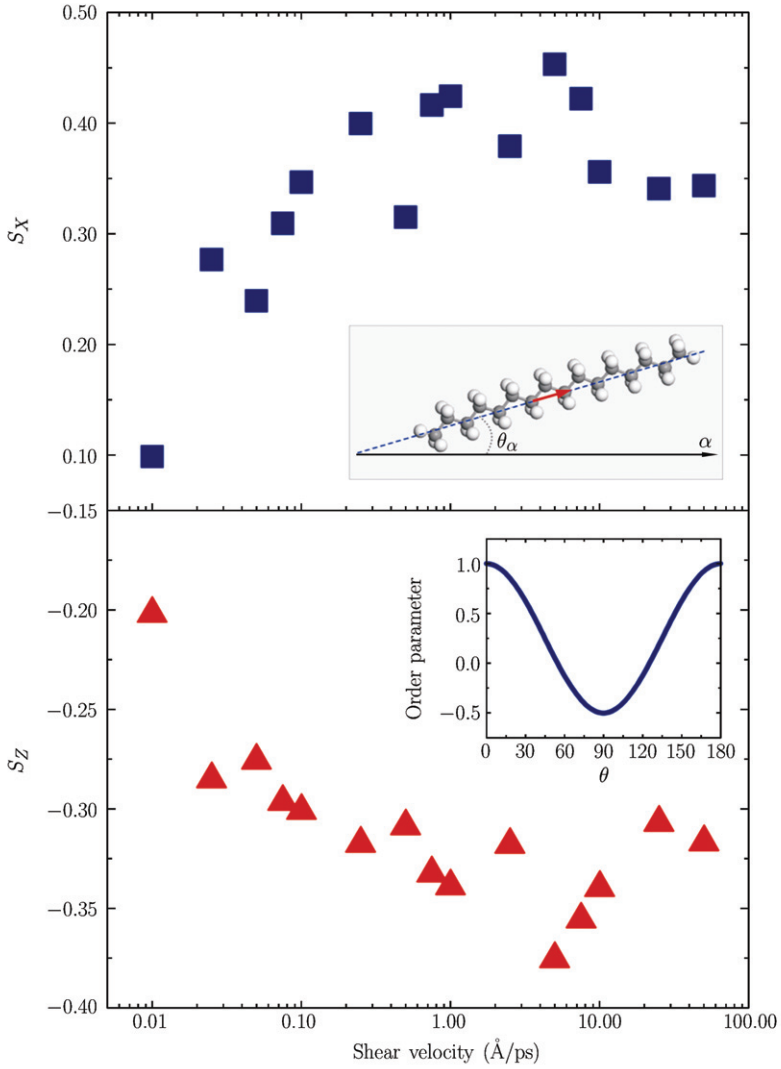

Fig. 6. Order parameter of the confined n-hexadecane molecules *vs*. different shear velocities. The arrow in the upper inset represents the chord vector which connects every other pair of carbon atoms in an n-hexadecane molecule. The lower inset describes the order parameter varies with the angle between the coordinate axes and the chord vectors.

3.4. Various Slip Regimes under Different Shear Velocities

It is now well-established that the liquid adjacent to a solid can slip. Martini et al. presented two mechanisms of slip, which were called defect slip and global slip, respectively[57]. In our simulations, a series of shear velocities were implied on the confined liquid, indicating different shear forces acting onto the liquid molecules. We found that slip first starts within the confined n-hexadecane liquid, since the liquid-liquid interactions are weaker than the liquid-solid interactions. As the shear velocity increases, slip also takes place at the liquid-solid interface. According to the velocity profiles shown in Fig.5 and other data not presented in the form of figures, we can divide the shear response of the confined n-hexadecane film into four stages:

(1) When the shear velocity is less than 0.25 Å/ps, the two layers of the n-hexadecane molecules stick to the adjacent Au walls. This is due to the strong adsorption interactions between the solid wall

and the confined liquid. The velocity profile of the middle layers is almost linear which can be predicted by the Navier-Stokes equations, as shown in Fig.5(a).

(2) When the shear velocity is between 0.25 Å/ps and 2.5 Å/ps, an intermediate state can be obtained. Slip starts between the two liquid layers (layers 1 and 2) near the lower wall while the layers 6 and 7 still stick to the upper wall, see Fig.5(b). The reason for the asymmetry of the velocity profile can be ascribed to that the initial configuration of the n-hexadecane is not extremely symmetrical in a strict sense.

(3) As the Au walls are sheared at velocities ranging from 2.5 Å/ps to 7.5 Å/ps, the stepwise velocity profiles show that obvious slip occurs within the confined liquid, between layers 1 and 2, as well as layers 6 and 7. Small velocity steps can also been observed at the middle of the film, illustrated in Fig.5(c).

(4) And afterwards, when the shear velocity is even higher than 7.5 Å/ps, slip occurs both at the liquid-wall interface and within the liquid, as shown in Fig.5(d).

Notably, the above results were summarized and schematically shown in Fig.7. It is clearly seen that slip first takes place at the middle of the confined liquid film and then expand to the liquid-solid interface as increasing the shear velocity. These various slip regimes proposed in our present work may lead to a new understanding of the slip boundary conditions for nanofluidics.

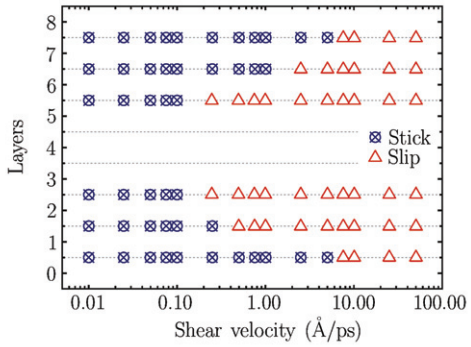

Fig. 7. Diagram of various slip regimes for the confined n-hexadecane liquid. The horizontal dash lines denote the dividing lines between liquid layers or the liquid/solid interface. The vertical ordinate denotes different layers of the confined n-hexadecane and the Au walls, which were illustrated in Fig.4. When a layer transition took place, layer 4 vanished.

3.5. Shear-thinning of the Individual Liquid Layer

Relaxation time is one of the key parameters to predict the dynamic properties of polymers and it has been discussed in many literatures[58,59]. It was suggested that the longest relaxation time of the confined n-hexadecane system is roughly the inverse of the transitional shear rate when the shear-thinning takes place[60]. When the shear rate exceeds certain critical value, the liquid molecules can not respond fast enough adjusting to the deformation due to shear, hence the confined liquid forms ordered structures which promotes the sliding motion between different layers, resulting in reduced viscosity, i.e., shear-thinning. Using the Rouse model[58], the relaxation time of n-hexadecane can be expressed as

$$\tau = \frac{6\eta_0 M}{\pi^2 \rho RT} \tag{8}$$

in which M is the molecular weight, ρ is the density of n-hexadecane at temperature T, R is the gas constant, the relaxation time of n-hexadecane was estimated to be 320 ps[60]. Additionally, the relaxation time of n-hexadecane at 300 K with the density of 0.770 g/cm^3 was determined to be 296 ps in MD simulations[16]. Consequently, our simulations on the timescale of several nanoseconds are long enough to probe the dynamics properties of n-hexadecane ultrathin films.

Shear-thinning occurs when the shear velocity exceeds the rate at which the confined liquid can relax the stress through rotational and translational molecular motions. The shear-thinning behavior has been

widely studied in the existing literatures[16, 25]. In this work, we mainly focus on the shear-thinning of the individual layers. The first and second layers adjacent to the Au walls were extracted as layers 1, 2, 6 and 7, while the left n-hexadecane liquid (layers 3-5) was incorporated into the middle layer. The viscosities of these five layers varying with different shear velocities are calculated according to Eqs.(5) and (6) and illustrated in Fig.8.

It can be concluded from Fig.8 that the viscosity of the confined n-hexadecane liquid varies with the distance from the solid wall, which is consistent with the interpretation of the experiments[42]. Viscosity of the liquid layers adjacent to the wall is much larger than that of the middle layers. All the liquid layers exhibit shear-thinning behavior when the shear velocity exceeds certain critical value, indicating that the relaxation time of the individual layer is different. As mentioned in the Introduction, the smaller the Weissenberg number, the more fluid the material appears. We can infer that the relaxation time of the middle liquid layers is shorter than that of the layers near the walls, namely, the middle liquid layers more mobile than the interfacial layers.

Shear-thinning behavior is normally accompanied by structural changes that reflect the fact that the confined liquid no longer has enough time to relax back to the equilibrium state[61]. The main structural change in our NEMD simulations has been presented in Figs.5 and 6. In constant load simulations, variation of the film thickness with shear rate has also been observed[22].

Comparing the viscosity curves in Fig.8 with the slip regimes in Fig.7, we can correlate the shear-thinning behavior of the individual layer with the sliding motion between liquid layers. There exists a competitive relationship between the shear force acting onto the confined liquid and its resistance to the deformation. When the shear velocity exceeds some certain value, sliding motion occurs and the viscosity of the respective layer decreases. The decreasing transition from the plateau region associated with the shear velocity at which the slip occurs. Moreover, as shown in Fig.8, the viscosity coefficients of layers 1 and 7 match approximately, while the viscosity of layers 2 and 6 exhibit deviation when the shear velocity is between 0.25 Å/ps and 2.5 Å/ps, which indicates the asymmetry development of slip illustrated in Fig.7. These results imply some kind of energy dissipation mechanism for confined ultrathin films under shear, which needs further investigations.

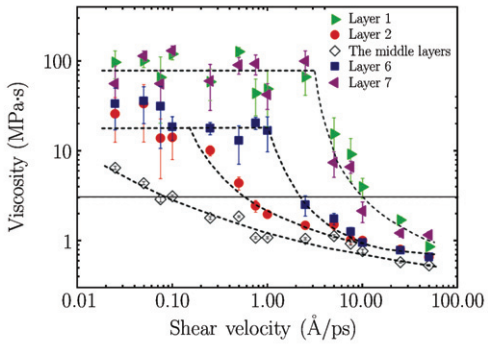

Fig. 8. Viscosity coefficients of different layers versus the shear velocities. The dash lines are guides to the eye. The Error bars are also shown. The layers 3-5 of n-hexadecane liquid were incorporated into the middle layer. The solid line which indicates the viscosity of the bulk n-hexadecane ($\sim$ 3.0 mPa·s at 300 K)[62] is displayed for comparison.

IV. CONCLUSIONS

In summary, the unique properties of the solid-like confined liquid films were reviewed in this presented work. Two kinds of the confined liquid, one is the simple liquid and the other one is n-hexadecane, were investigated using MD simulations. For the confined simple liquid, the thickness dependent of the liquid structure and the shear viscosity was discussed. A series of MD simulations were performed and the total number of the atoms reaches up to 102 million. As far as we are aware, this is the largest scale MD simulation performed in China. Shear velocity dependent of the dynamic response of the confined n-hexadecane ultrathin films were studied using full-atom NEMD simulations. When the shear velocity

increases, the confined n-hexadecane trend to be more ordered, and the layering structures have a drastic influence on the shear response. Slip occurs first within the confined liquid film and then expanded to the liquid-solid interface as the shear velocity increases. Our results also revealed that the viscosity of the liquid layer adjacent to the solid walls is much larger than that of the intermediate liquid.

As the film thickness comes to the nanometer scale, the validity of the continuum theory becomes questionable. Although the large-scale MD simulation can be performed, it is still time consuming for engineering applications. Future direction for this work is to develop a theoretical framework for the confined liquid, which should be suitable for the simple liquid, polar liquid such as water, and complicated liquid such as alkcane. Moreover, a multi-scale simulation investigation is undergoing.

References

[1] White,F.M., Fluid Mechanics. New York: McGraw-Hill, 1994.

[2] Granick,S., Motions and relaxations of confined liquids. *Science*, 1991, 253: 1374-1379.

[3] Horn,R.G. and Israelachvili,J.N., Direct measurement of structural forces between two surfaces in a nonpolar liquid. *Journal of Chemical Physics*, 1981, 75: 1400-1411.

[4] Heuberger,H., Zach,M. and Spencer,N.D., Density fluctuations under confinement: when is a fluid not a fluid? *Science*, 2001, 292: 905-908.

[5] Gee,M.L., McGuiggan,P.M., Israelachvili1,J.N. and Homola,A.M., Liquid to solidlike transitions of molecularly thin films under shear. *Journal of Chemical Physics*, 1990, 93: 1895-1906.

[6] Zhu,Y.X. and Granick,S., Superlubricity: a paradox about confined fluids resolved. *Physical Review Letters*, 2004, 93: 096101.

[7] Bhushan,B., Israelachvili,J.N. and Landman,U., Nanotribology: friction, wear and lubrication at the atomic scale. *Nature*, 1995, 374: 607-616.

[8] Demirel,A.L. and Granick,S., Origins of solidification when a simple molecular fluid is confined between two plates. *Journal of Chemical Physics*, 2001, 115: 1498-1512.

[9] Mukhopadhyay,A., Bae,S.C., Zhao,J. and Granick,S., How confined lubricants diffuse during shear. *Physical Review Letters*, 2004, 93: 236105.

[10] Karniadakis,G., Beskok,A. and Aluru,N., Microflows and Nanoflows: Fundamentals and Simulation. New York: Springer, 2005.

[11] Yuan,Q.Z. and Zhao,Y.P., Hydroelectric voltage generation based on water-filled single-walled carbon nanotubes. *Journal of the American Chemical Society*, 2009, 131: 6374-6376.

[12] Qin,X.C., Yuan,Q.Z., Zhao,Y.P., Xie,S.B. and Liu,Z.F., Measurement of the rate of water translocation through carbon nanotubes. *Nano Letters*, 2011, dx.doi.org/10.1021/nl200843g.

[13] McGuiggan,P.M., Gee,M.L., Yoshizawa,H., Hirz,S.J. and Israelachvili,J.N., Friction studies of polymer lubricated surfaces. *Macromolecules*, 2007, 40(6): 2126-2133.

[14] Lim,R., Li,S.F.Y. and O'Shea,S.J., Solvation forces using sample-modulation atomic force microscopy. *Langmuir*, 2002, 18: 6116-1624.

[15] Patil,S., Mater,G., Oral,A. and Hoffmann,P.M., Solid or liquid? solidification of a nanoconfined liquid under nonequilibrium conditions. *Langmuir*, 2006, 22: 6485-6488.

[16] Cui,S.T., Gupta,S.A., Cummings,P.T. and Cochran,H.D., Molecular dynamics simulations of the rheology of normal decane, hexadecane, and tetracosane. *Journal of Chemical Physics*, 1996, 105: 1214-1220.

[17] Gao,J.P., Luedtke,W.D. and Landman,U., Origins of solvation forces in confined films. *Journal of Physical Chemistry B*, 1997, 101: 4013-4023.

[18] Israelachvili,J.N., Intermolecular and Surface Forces. San Diego: Academic Press, 1992.

[19] Yin,J. and Zhao,Y.P., Hybrid QM/MM simulation of the hydration phenomena of dipalmitoylphosphatidylcholine headgroup. *Journal of Colloid and Interface Science*, 2009, 329: 410-415.

[20] Yang,C.Y. and Zhao,Y.P., Influences of hydration force and elastic strain energy on stability of solid film in very thin solid-on-liquid structure. *Journal of Chemical Physics*, 2004, 120: 5366-5376.

[21] Yamada,S., Layering transitions and tribology of molecularly thin films of poly(dimethylsiloxane). *Langmuir*, 2003, 19: 7399-7405.

[22] Jabbarzadeh,A., Harrowell,P. and Tanner,R.I., Very low friction state of a dodecane film confined between mica surfaces. *Physical Review Letters*, 2005, 94: 126103.

[23] Jabbarzadeh,A., Harrowell,P. and Tanner,R.I., Crystal bridge formation marks the transition to rigidity in a thin lubrication film. *Physical Review Letters*, 2006, 96: 206102.

[24] Bureau,L., Rate effects on layering of a confined linear alkane. *Physical Review Letters*, 2007, 99: 225503.

[25] Cui,S.T., McCabe,C., Cummings,P.T. and Cochran,H.D., Molecular dynamics study of the nano-rheology of n-dodecane confined between planar surfaces. *Journal of Chemical Physics*, 2003, 118: 8941-8944.

[26] Reiner,M., The Deborah number. *Physics Today*, 1964, 17: 62.
[27] Landau,L.D. and Lifshitz,E.M., Theory of Elasticity. Oxford: Butterworth-Heinemann, 1999.
[28] Kumacheva,E. and Klein,J., Simple liquids confined to molecularly thin layers. II. Shear and frictional behavior of solidified films. *Journal of Chemical Physics*, 1998, 108: 7010-7022.
[29] Khan,S.H., Matei,G., Patil,S. and Hoffmann,P.M., Dynamic solidification in nanoconfined water films. *Physical Review Letters*, 2010, 105: 106101.
[30] Bureau,L., Nonlinear rheology of a nanoconfined simple fluid. *Physical Review Letters*, 2010, 104: 218302.
[31] Granick,S., Bae,S.C., Kumar,S. and Yu,C., Confined liquid controversies near closure? *Physics*, 2010, 3: 73.
[32] Huang,D.M., Sendner,C., Horinek,D., Netz,R.R. and Bocquet,L., Water slippage versus contact angle: a quasiuniversal relationship. *Physical Review Letters*, 2008, 101: 226101.
[33] Granick,S., Lee,H. and Zhu,Y., Slippery questions of stick when fluid flows past surfaces. *Nature Materials*, 2003, 2: 221-227.
[34] De Gennes,P.G., On fluid/wall slippage. *Langmuir*, 2002, 18: 3413-3414.
[35] Thompson,P.A. and Troian,S.M., A general boundary condition for liquid flow at solid surfaces. *Nature*, 1997, 389: 360-362.
[36] Lauga, E., Apparent slip due to the motion of suspended particles in flows of electrolyte solutions. *Langmuir*, 2004, 20: 8924-8930.
[37] Schmatko,T., Hervet,H. and Leger,L., Friction and slip at simple fluid-solid interfaces: the roles of the molecular shape and the solid-liquid interaction. *Physical Review Letters*, 2005, 94: 244501.
[38] Vinogradova,O.I., Slippage of water over hydrophobic surfaces. *International Journal of Mineral Processing*, 1999, 56: 31-60.
[39] Jabbarzadeh,A., Atkinson,J.D. and Tanner,R.I., Wall slip in the molecular dynamics simulation of thin films of hexadecane. *Journal of Chemical Physics*, 1999, 110: 2612-2620.
[40] Jabbarzadeh,A., Atkinson,J.D. and Tanner,R.I., Effect of the wall roughness on slip and rheological properties of hexadecane in molecular dynamics simulation of Couette shear flow between two sinusoidal walls. *Physical Review E*, 2000, 61: 690-699.
[41] Pit,R., Hervet,H. and Leger,L., Direct experimental evidence of slip in hexadecane: solid interfaces. *Physical Review Letters*, 2000, 85: 980-983.
[42] Zhu,Y.X. and Granick,S., Rate-dependent slip of Newtonian liquid at smooth surfaces. *Physical Review Letters*, 2001, 87: 096105.
[43] Plimpton,S., Fast parallel algorithms for short-range molecular-dynamics. *Journal of Computational Physics*, 1995, 117: 1-19.
[44] Berendsen,H.J.C., Grigera,J.R. and Straatsma,T.P., The missing term in effective pair potentials. *Journal of Physical Chemistry*, 1987, 91: 6269-6271.
[45] Hoover,W.G., Canonical dynamics: equilibrium phase-space distributions. *Physical Review A*, 1985, 31: 1695-1697.
[46] Stuart,S.J., Tutein,A.B. and Harrison,J.A., A reactive potential for hydrocarbons with intermolecular interactions. *Journal of Chemical Physics*, 2000, 112: 6472-6486.
[47] Halicioglu,T. and Pound,G.M., Calculation of potential energy parameters from crystalline state properties. *Physica Status Solidi A: Applied Research*, 1975, 30: 619-623.
[48] Dauberosguthorpe,P., Roberts,V.A., Osguthorpe,D.J., Wolff,J., Genest,M. and Hagler,A.T., Structure and energetics of ligand binding to proteins: escherichia coli dihydrofolate reductase-trimethoprim, a drug-receptor system. *Proteins-Structure Function and Genetics*, 1988, 4: 31-47.
[49] Ardekani,A.M. and Joseph,D.D., Instability of stationary liquid sheets. *Proceedings of the National Academy of Sciences of the United States of America*, 2009, 106: 4992-4996.
[50] De Gennes,P.G., Brochard-Wyart,F. and Quere,D., Capillarity and Wetting Phenomena. New York: Springer, 2004.
[51] Brochard-Wyart,F., Raphael,E. and Vovelle,L., Démouillage en régime inertiel: apparitions d'ondes capillaries. *Comptes Rendus de l'Académie des Sciences*, 1995, 321: 367-370.
[52] Wang,F.C., Feng,J.T. and Zhao,Y.P., The head-on colliding process of binary liquid droplets at low velocity: High-speed photography experiments and modeling. *Journal of Colloid and Interface Science*, 2008, 326: 196-200.
[53] Yuan,Q.Z. and Zhao,Y.P., Precursor film in dynamic wetting, electrowetting and electro-elasto-capillarity. *Physical Review Letters*, 2010, 104: 246101.
[54] Li,J., AtomEye: an efficient atomistic configuration viewer. *Modelling and Simulation in Materials Science and Engineering*, 2003, 11: 173-177.
[55] Jabbarzadeh,A. and Tanner,R.I., Crystallization of alkanes under quiescent and shearing conditions. *Journal of Non-Newtonian Fluid Mechanics*, 2009, 160: 11-21.

[56] Drummond,C., Alcantar,N. and Israelachvili,J., Shear alignment of confined hydrocarbon liquid films. *Physical Review E*, 2002, 66: 011705.
[57] Martini,A., Roxin,A., Snurr,R.Q., Wang,Q. and Lichter,S., Molecular mechanisms of liquid slip. *Journal of Fluid Mechanics*, 2008, 600: 257-269.
[58] Doi,M. and Edwards,S.F., The Theory of Polymer Dynamics. Oxford: Calderon Press, 1986.
[59] Yin,J., Zhao,Y.P. and Zhu,R.Z., Molecular dynamics simulation of barnacle cement. *Materials Science and Engineering A*, 2005, 409: 160-166.
[60] Berker,A., Chynoweth,S., Klomp,U.C. and Michopoulos,Y., Non-equilibrium molecular dynamics (NEMD) simulations and the rheological properties of liquid n-hexadecane. *Journal of the Chemical Society-Faraday Transactions*, 1992, 88: 1719-1725.
[61] Thompson,P.A., Robbins,M.O. and Grest,G.S., Structure and shear response in nanometer thick films. *Israel Journal of Chemistry*, 1995, 35: 93-106.
[62] Wohlfarth,C. and Wohlfahrt,B., Pure Organic Liquids. New York: Springer, 2002.